

## Electronic Supplementary Material:

### High Electron Mobility, Controllable Magnetism and Anomalous Light Absorption in Monolayered Tin Mononitride Semiconductor

Shuqing Zhang and Xiaolong Zou\*

*Shenzhen Geim Graphene Center (SGC), Tsinghua-Berkeley Shenzhen Institute (TBSI)  
& Tsinghua Shenzhen International Graduate School (TSIGS), Tsinghua University,  
Shenzhen 518055, China*

\* Corresponding author (email: [xlzou@sz.tsinghua.edu.cn](mailto:xlzou@sz.tsinghua.edu.cn))

**Band structures for various 2D pnictides.** Fig. S1 shows the calculated band structures for SiN, GeN, SnN, PbN, SiP, GeP, SnP and PbP monolayers by using PBE functional,<sup>1</sup> which is well suited for the rapid screening of materials because of its efficiency, but it systematically underestimates band gaps of materials. Generally, the band gap calculated by PBE method may be underestimated by about 0.5~1 eV. If we add the difference to band gaps of these materials, the values of SnN and PbP will be in the range of solar absorption. Given toxicity of Pb atom, we only focus on the novel properties of SnN.

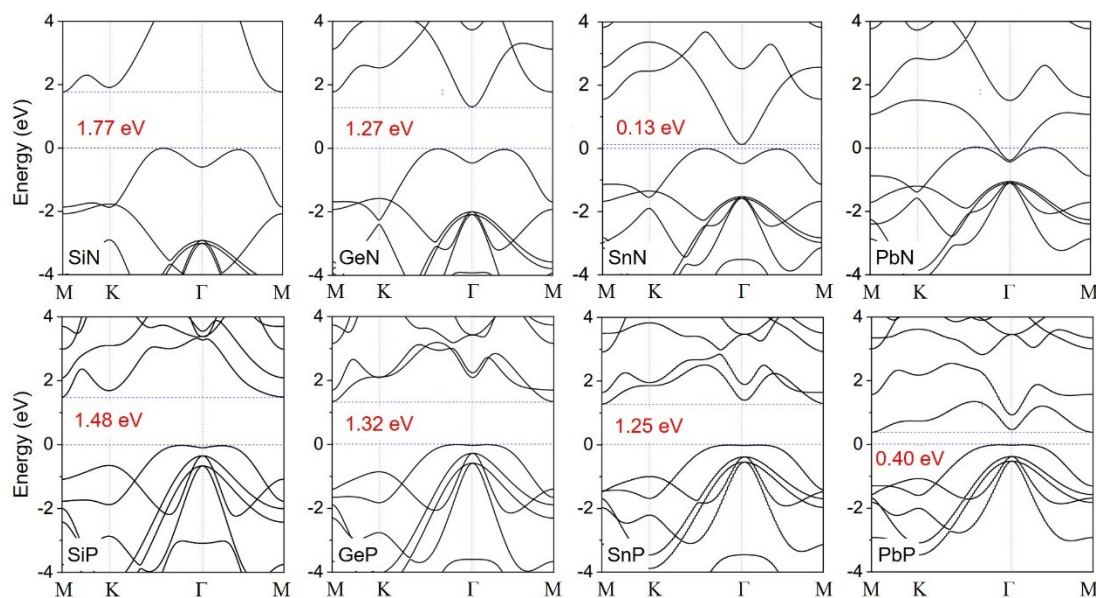


Fig. S1 Band structures of SiN, GeN, SnN, PbN, SiP, GeP, SnP and PbP monolayers at the PBE level.

**Exfoliation energy of SnN monolayer.** The mechanical exfoliation is the simplest approach to obtain 2D materials from their bulk crystals thanks to weak van der Waals

interlayer binding in layered materials. We calculate the exfoliation process of SnN monolayer from the surface of its layered bulk crystal, which is simulated by a five-layer sample. The calculated exfoliation energy for graphite is  $0.30 \text{ J m}^{-2}$  by this method, comparable to experimental values of  $0.18\text{-}0.35 \text{ J m}^{-2}$ .<sup>2-4</sup> Fig. S2 demonstrate that the exfoliation energy of SnN monolayer is about  $0.69 \text{ J m}^{-2}$ , which is much less than other newly reported atomic-layered pnictides, such as exfoliation energies for  $\text{Ca}_2\text{N}$ <sup>5</sup>,  $\text{InP}_3$ <sup>6</sup>,  $\text{GeP}_3$ <sup>7</sup> and  $\text{GaP}_3$ <sup>8</sup> are 1.08, 1.32, 1.14 and  $1.30 \text{ J m}^{-2}$ , respectively. The relatively small exfoliation energy of SnN monolayer imply that it is feasible to cleavage from its bulk form.

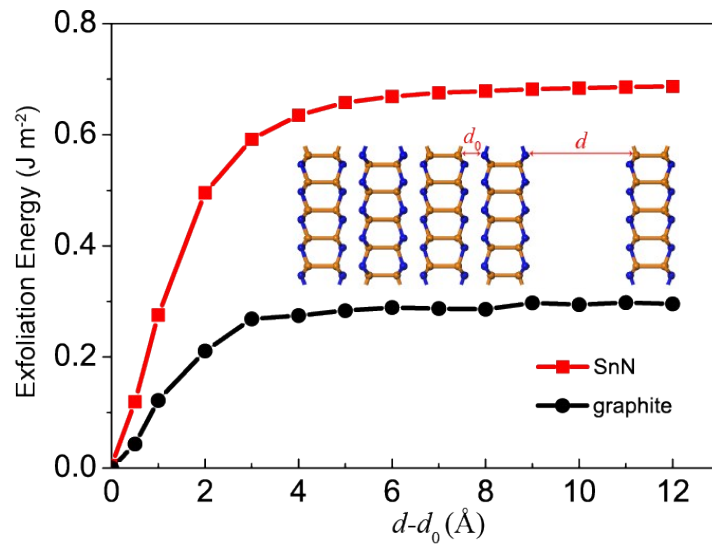


Fig. S2 Exfoliation energy of SnN monolayer, calculated by enlarging the distance of monolayer from the slab of five layers, which resembles bulk model.

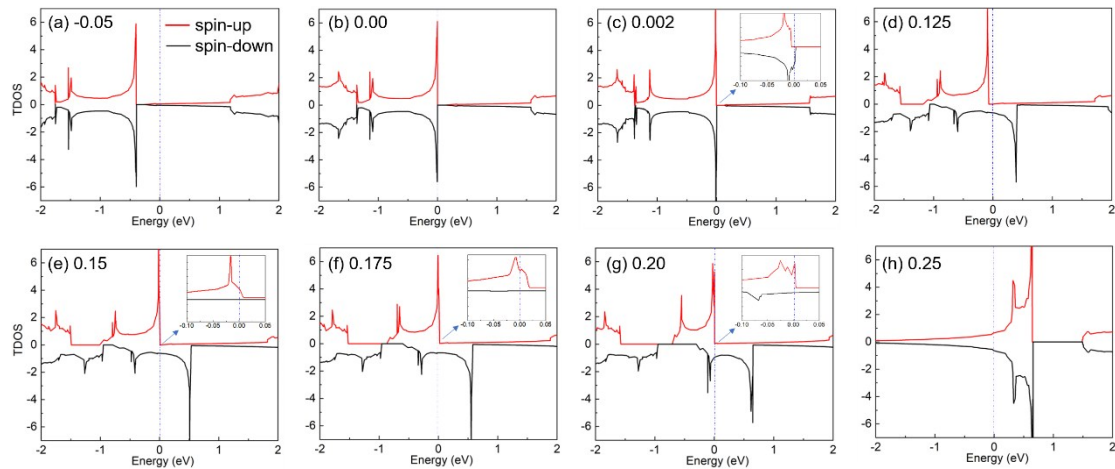


Fig. S3 (a-h) Total density of states (TDOS) of SnN monolayer with different doping concentrations. Insets are enlarged view around Fermi energy, which is set to 0 eV. Negative and positive numbers in subplots correspond to electron and hole doping, and their units are

doped carrier/atom. Nonmagnetic states are also represented by spin-up and spin-down channels for comparison with ferromagnetic states.

Fig. S3 shows the TDOS of SnN monolayer with different doping concentrations. For electron doping (Fig. S3a), the system remains nonmagnetic with equal occupations in spin-up and spin-down electrons. For systems with doping concentration from 0.002 hole/atom to 0.125 hole/atom (Fig. S3b, Fig. S3c), they show half-metallic DOS, where doped holes only occupy spin-down bands, leading to 100% spin polarization percentage  $P$  ( $P$  is proportional to the difference between the number of spin-up states and that of spin-down states at Fermi level). When the doping concentration increases to 0.15 hole/atom (Fig. S3e), the Fermi level begins to cross the spin-up bands as well, because the decreased DOS in spin-down channel cannot hold all the doped holes. This results in a reduction in spin polarization and magnetic moment as well. As the doping concentration increases to 0.175 hole/atom (Fig. S3f), the number of unoccupied spin-up states above Fermi level increases, and the spin polarization percentage is further reduced. As a result, the magnetic moment shows a one-tenth reduction in Fig. 4. When the doping density increases to 0.2 hole/atom, the Fermi level further moves down in energy. Meanwhile, the spin-down DOS increases significantly, and the doped holes again mainly occupy the spin-down channel (Fig. S3h). Accordingly, the magnetic moment increases to  $1\mu_B/\text{carrier}$ . After that, the large VHS peak in spin-up channel starts to play a key role, and the magnetic moment falls steeply to zero with increasing hole doping.

## Reference

1. J. P. Perdew, K. Burke, and M. Ernzerhof, *Phys. Rev. Lett.* 1996, **77**, 3865-3868.
2. R. Zacharia, H. Ulbricht, and T. Hertel, *Phys. Rev. B* 2004, **69**, 155406.
3. Z. Liu, J. Z. Liu, Y. Cheng, Z. Li, L. Wang, and Q. Zheng, *Phys. Rev. B* 2012, **85**, 205418
4. Y. Yamashita, H. Yakiwara, Y. Asano, H. Shimizu, K. Uchida, S. Hirano, K. Umakoshi, H. Miyamachi, M. Nakamoto, M. Fukui, M. Kamizono, H. Kanehara, T. Yamada, M. Shinohara, and K. Obara, *Science* 2015, **348**, 676-679.
5. S. Zhao, Z. Li, and J. Yang, *J. Am. Chem. Soc.* 2014, **136**, 13313-13318.
6. N. Miao, B. Xu, N. C. Bristowe, J. Zhou, and Z. Sun, *J. Am. Chem. Soc.* 2017, **139**, 11125-11131.
7. Y. Jing, Y. Ma, Y. Li, and T. Heine, *Nano Lett.* 2017, **17**, 1833-1838.
8. N. Lu, Z. Zhuo, H. Guo, P. Wu, W. Fa, X. Wu, and X. C. Zeng, *J Phys Chem Lett* 2018, **9**, 1728-1733.